Optics Communications 367 (2016) 95–101

Contents lists available at ScienceDirect

Optics Communications

journal homepage: www.elsevier.com/locate/optcom

Broadening of ultra-short pulses propagating through weak-to-strong oceanic turbulence

Zhiqiang Wang [a,b], Lu Lu [a,b,*], Pengfei Zhang [a], Chengyu Fan [a,**], Xiaoling Ji [c]

[a] Key Laboratory of Atmospheric Composition and Optical Radiation, Anhui Institute of Optics and Fine Mechanics, Chinese Academy of Sciences, Hefei 230031, China
[b] University of Science and Technology of China, Hefei 230026, China
[c] Department of Physics, Sichuan Normal University, Chengdu 610066, China

ARTICLE INFO

Article history:
Received 4 October 2015
Received in revised form
2 January 2016
Accepted 7 January 2016
Available online 4 February 2016

Keywords:
Ultra-short pulses
Two-frequency mutual coherence function
Pulse width
Oceanic turbulence
Rytov variance
On-axis relative pulse broadening and turbulent effective coefficient

ABSTRACT

In this paper, the new approach of correlation function of the complex phase perturbed by oceanic turbulence is shown. Based on this new approach, the general formula of the two-frequency mutual coherence function (MCF) of ultra-short pulses in oceanic turbulence is derived. Using a temporal moments approach and combining with this new formula for the MCF, the analytical expression for the pulse width is deduced. Besides, the quantity of Rytov variance σ_R^2 in oceanic turbulence is obtained, which is widely used as a measure of the strength of turbulence. In particular, the on-axis relative pulse broadening and turbulent effective coefficient of ultra-short pulses (i.e., femtosecond–picosecond regime) propagating through oceanic turbulence are investigated.

1. Introduction

One of the major advantages optical communication systems have over conventional radio frequency (RF) systems is their high antenna gain, which allows for higher data transmission rates. However, due to the shorter wavelengths used in optical communication systems, the optical pulse experiences degradation as it passes through atmospheric turbulence. These effects result in higher bit error rates (BER) and diminish the performance of an optical communication system [1]. Until now, some works have been carried out concerning the temporal broadening of pulse beam in atmospheric turbulence based on various turbulent models, such as, von Karman [2], modified von Karman [1], Kolmogorov [3], non-Kolmogorov [3] spectrum and etc. Recently, characterization of temporal pulse broadening for horizontal propagation in strong anisotropic atmospheric turbulence has already been studied [4]. Due to the complexity of oceanic turbulence, pulse beam propagating through oceanic turbulence is relatively less explored compared to that in atmospheric turbulence. The propagation of an ultra-short pulse of light through a linear and absorptive medium such as water, is of great fundamental importance for several reasons. One of the most important of which is that it may be possible to transmit information over much greater distances using ultra-short pulses compared to propagation distances achieved by using pulses with long time durations, including CW (continuous waves) [5]. The first measurements which claimed to observe optical precursors in deionized water were made by Choi and Österberg [6] where they found that the precursors were attenuated non-exponentially with distance. Hence, an understanding of these degrading effects is imperative in seawater. As we know, the two frequency mutual coherence function (MCF) benefits to deduce the temporal broadening. It is essential to obtain an analytical expression for the two-frequency MCF related to oceanic turbulence. In the past decades, many researchers have independently studied the two-frequency MCF [2–4,7–12]. Young has researched the two-frequency MCF and Gaussian pulse broadening in weak atmospheric turbulence based on weak fluctuation theory [12], while Young and co-workers have also studied the two-frequency MCF and the percent broadening of ultra-short optical pulses in moderate to strong atmospheric turbulence [2]. However, there has been no formulation concerning both the two-frequency MCF and the

* Corresponding author at: Key Laboratory of Atmospheric Composition and Optical Radiation, Anhui Institute of Optics and Fine Mechanics, Chinese Academy of Sciences, Hefei 230031, China/University of Science and Technology of China.
** Corresponding author.
E-mail addresses: luquanchengll@sina.com (L. Lu), cyfan@aiofm.ac.cn (C. Fan).

http://dx.doi.org/10.1016/j.optcom.2016.01.013
0030-4018/

pulse width of optical pulses propagating through oceanic turbulence. Therefore, a deep investigation on this problem is imperative. In this paper, we generally formulate two-frequency MCF based on the extended Huygens–Fresnel principle which is valid in various strength of oceanic turbulence and the new approach of correlation function of the complex phase perturbed by oceanic turbulence. In arriving at the results, an analytical expression for the pulse width of optical pulses transmitting through oceanic turbulence is obtained. Based on the quantity of Rytov variance for a plane wave in oceanic turbulence, we also investigate the on-axis relative pulse broadening and turbulent effective coefficient with the propagation length, wavelength, initial pulse half-width and the initial beam radius from weak to strong turbulence.

2. Oceanic turbulence

Since the power spectrum of oceanic turbulence proposed by Nikishov et al. [13], there has been remarkable interest in the study of propagation characteristics using laser beams in seawater. The power spectrum of oceanic turbulence has been simplified for homogeneous and isotropic water media in Ref. [14]. According to Ref. [13], when the eddy thermal diffusivity and the diffusion of salt are assumed to be equal, the power spectrum for homogeneous and isotropic oceanic water is given by:

$$\Phi_n(\kappa) = 0.388\times 10^{-8}\varepsilon^{-1/3}\kappa^{-11/3}[1+2.35(\kappa\eta)^{2/3}]\frac{\chi_T}{w^2}(w^2e^{-A_T\delta} + e^{-A_S\delta} - 2we^{-A_{TS}\delta}), \quad (1)$$

where ε is the rate of dissipation of kinetic energy per unit mass of fluid ranging from $10^{-1}\mathrm{m}^2/\mathrm{s}^3$ to $10^{-10}\mathrm{m}^2/\mathrm{s}^3$, χ_T is the rate of dissipation of mean-squared temperature and has the range $10^{-4}\mathrm{K}^2/\mathrm{s}$ to $10^{-10}\mathrm{K}^2/\mathrm{s}$, w defines the ratio of temperature and salinity contributions to the refractive index spectrum, which varies in the interval $[-5;\ 0]$, with -5 and 0 corresponding to dominating temperature-induced and salinity-induced optical turbulence, respectively [15]. Additionally, η is the Kolmogorov micro scale (inner scale), and $A_T = 1.863\times 10^{-2}$, $A_S = 1.9\times 10^{-4}$, $A_{TS} = 9.41\times 10^{-3}$, $\delta = 8.284(\kappa\eta)^{4/3} + 12.978(\kappa\eta)^2$ [15].

3. Two frequency MCF

3.1. Formulae

Let us consider a temporal Gaussian input pulse applied at the transmitter and propagated through the oceanic turbulence to a receiver located at distance L from the transmitter, and assume the input pulse is the modulated signal with the carrier frequency ω_0 that can be represented by [16].

$$p_i(t) = v_i(t)\exp(-\mathrm{i}\omega_0 t), \quad (2)$$

where the amplitude $v_i(t) = \exp(-t^2/T_0)$ represents the pulse shape, and T_0 is the initial pulse half-width. Here, we introduce the Fourier transform of the input pulse by the expression [16].

$$\begin{aligned} P_i(\omega) &= \int_{-\infty}^{\infty} p_i(t)\exp(\mathrm{i}\omega t)dt \\ &= \int_{-\infty}^{\infty} v_i(t)\exp(-\mathrm{i}\omega_0 t)\exp(\mathrm{i}\omega t)dt \\ &= V_i(\omega-\omega_0), \end{aligned} \quad (3)$$

where $V_i(\omega)$ is the Fourier transform of the amplitude $v_i(t)$. Similarly, $p_o(t) = v_o(t)\exp(-\mathrm{i}\omega_0 t)$ and $P_o(\omega) = V_o(\omega-\omega_0)$ represent the output pulse at the receiver and the Fourier transform of output, respectively.

The single-point, two-frequency correlation function of the complex envelop of the output pulse is defined by the ensemble average [12].

$$B_v(\mathbf{r},\mathbf{r},L;t_1,t_2) = \frac{1}{(2\pi)^2}\int_{-\infty}^{\infty}\int_{-\infty}^{\infty} V_i(\omega_1)V_i^*(\omega_2)\Gamma_2(\mathbf{r},\mathbf{r},L;\omega_1,\omega_2) \exp(-\mathrm{i}\omega_1 t_1 + \mathrm{i}\omega_2 t_2)\mathrm{d}\omega_1\mathrm{d}\omega_2, \quad (4)$$

where the Fourier transform of input Gaussian pulse is

$$V_i(\omega) = \sqrt{\pi}T_0\exp\left(-\frac{1}{4}\omega^2T_0^2\right), \quad (5)$$

and the two-frequency MCF is

$$\Gamma_2(\mathbf{r},\mathbf{r},L;\omega_1,\omega_2) = \langle U(\mathbf{r},L;\omega_1+\omega_0)U^*(\mathbf{r},L;\omega_2+\omega_0)\rangle. \quad (6)$$

Here $U(\bullet)$ is the complex amplitude of the wave in oceanic turbulence, $\mathbf{r}$ is the position vector in the transverse plane at propagation distance L from the source.

In particular, using the extended Huygens–Fresnel principle, $U(\bullet)$ in Eq. (6) can be written by

$$U(\mathbf{r},L;\omega) = -\frac{\mathrm{i}\omega}{2\pi Lc}\exp\left(\frac{\mathrm{i}L\omega}{c}\right)\int_{-\infty}^{\infty}\mathrm{d}^2\mathbf{r}_1 U_0(\mathbf{r}_1,0;\omega)\exp\left[\frac{\mathrm{i}\omega|\mathbf{r}_1-\mathbf{r}|^2}{2Lc} + \psi(\mathbf{r}_1,\mathbf{r},L;\omega)\right], \quad (7)$$

where c is the speed of light, $U_0(\mathbf{r},0;\omega) = \exp[-\mathbf{r}^2/W_0^2]$ denotes the optical wave field in the source plane, $\psi(\bullet)$represents the random part of the complex phase of a spherical wave due to the turbulence [16].

On substituting Eq. (7) into Eq. (6), we obtain the expression of MCF in oceanic turbulence, i.e.,

$$\Gamma_2(\mathbf{r},\mathbf{r},L;\omega_1,\omega_2) = \frac{\omega_1\omega_2}{4\pi^2L^2c^2}\exp\left[\frac{\mathrm{i}L(\omega_1-\omega_2)}{c}\right]\int_{-\infty}^{\infty}\mathrm{d}^2\mathbf{r}_1\int_{-\infty}^{\infty}\mathrm{d}^2\mathbf{r}_2 U_0(\mathbf{r}_1,0;\omega_1)U_0(\mathbf{r}_2,0;\omega_2) \times\exp\left[\frac{\mathrm{i}\omega|\mathbf{r}_1-\mathbf{r}|^2}{2Lc} - \frac{\mathrm{i}\omega|\mathbf{r}_2-\mathbf{r}|^2}{2Lc}\right] \langle\exp[\psi(\mathbf{r}_1,\mathbf{r},L;\omega_1) + \psi^*(\mathbf{r}_2,\mathbf{r},L;\omega_2)]\rangle_m, \quad (8)$$

where $<\bullet>_m$ denotes average over the ensemble of the turbulent medium [16], $\mathbf{r}_m$ $(m=1,\ 2)$ is a position vector of a point in the source plane, and the correlation function of the complex phase perturbed by oceanic turbulence.

$$\langle\exp[\psi(\mathbf{r}_1,\mathbf{r},L;\omega_1) + \psi^*(\mathbf{r}_2,\mathbf{r},L;\omega_2)]\rangle_m = \left(\frac{2\pi}{c}\right)^2L\int_0^{\infty}\mathrm{d}\kappa\kappa\Phi_n(\kappa)\int_0^1\mathrm{d}\xi\left[\omega_1^2+\omega_2^2-2\omega_1\omega_2J_0\left(\kappa\xi|\mathbf{r}_2-\mathbf{r}_1|\right)\right], \quad (9)$$

where $J_0(\bullet)$ is the Bessel function of the first kind and order zero. κ is the magnitude of spatial wavenumber.

In this paper, the quadratic approximation in Rytov's phase structure function (i.e., $\left\langle\exp[\psi(\mathbf{r}_1,\mathbf{r},L;\omega_1) + \psi^*(\mathbf{r}_2,\mathbf{r},L;\omega_2)]\right\rangle_m \cong \exp[-(\mathbf{r}_1-\mathbf{r}_2)^2/\rho_0^2]$) [17–22] and second order approximation (i.e., $J_0(\kappa\xi|\mathbf{r}_2-\mathbf{r}_1|) \approx 1-\kappa^2\xi^2|\mathbf{r}_2-\mathbf{r}_1|^2/4$) [23–25] have not been used in Eq. (9). Replacing $J_0(\bullet)$ in Eq. (9) by $J_0(\kappa\xi|\mathbf{r}_2-\mathbf{r}_1|) = \sum_{n=0}^{\infty}\frac{(-1)^n(\kappa\xi|\mathbf{r}_2-\mathbf{r}_1|/2)^{2n}}{n!\,\Gamma(n+1)}$ [26], and after some mathematical manipulations, it follows that

$$\Gamma_2(\mathbf{r}, \mathbf{r}, L; \omega_1, \omega_2) = \frac{\omega_1\omega_2}{L^2c^2(4a_1a_2 - \omega_1^2\omega_2^2E^2)} \exp\left[\frac{\mathrm{i}L(\omega_1 - \omega_2)}{c}\right] \exp\left[\frac{\mathrm{i}(\omega_1 - \omega_2)\mathrm{r}^2}{2Lc}\right] \times \exp\left[-\frac{D}{2}(\omega_1 - \omega_2)^2\right] \exp\left[-\frac{\mathrm{r}^2}{4L^2c^2a_1}\frac{\left(2a_1\omega_2 + \omega_1^2\omega_2E\right)^2}{4a_1a_2 - \omega_1^2\omega_2^2E^2}\right] \exp\left[-\frac{\omega_1^2\mathrm{r}^2}{4L^2c^2a_1}\right]. \tag{10}$$

where

$$a_1 = \frac{1}{W_0^2} - \frac{\omega_1\omega_2E}{2} - \frac{\mathrm{i}\omega_1}{2Lc},\ a_2 = \frac{1}{W_0^2} - \frac{\omega_1\omega_2E}{2} + \frac{\mathrm{i}\omega_2}{2Lc},\ D = 0.388 \times 10^{-8}\left(\frac{2\pi}{c}\right)^2 L\varepsilon^{-1/3}\frac{\chi_T}{w^2}(3.07 \times 10^{-5}w^2 - 4.07 \times 10^{-5}w + 2.29 \times 10^{-6}),\ E = 0.388 \times 10^{-8}\left(\frac{2\sqrt{2}\pi}{c}\right)^2 L\varepsilon^{-1/3}\frac{\chi_T}{w^2}(1.116w^2 - 2.235w + 1.119). \tag{11}$$

and W_0 is the initial beam radius of the Gaussian beam.

3.2. Numerical calculation results and analysis

Due to the previous research, the quadratic approximation in Rytov's phase structure function [17–22] and the second order approximation [23–25] have been widely used in Eq. (9). Expanding the zero-order Bessel function directly is the new approach in this paper. In this section, the relation of three approaches is analyzed. Assuming $\omega_1 = \omega_2$, taking the propagation distance for example, the relation between $\left\langle \exp[\psi(\mathbf{r_1}, \mathbf{r}, L; \omega_1) + \psi^*(\mathbf{r_2}, \mathbf{r}, L; \omega_2)]\right\rangle_m$ and propagation distance is plotted in Fig. 1. From Fig. 1, it is shown that the result of the second order approximation is much larger than that of other approaches. Besides, the new approach is close to quadratic approximation in Rytov's phase structure function. In atmospheric turbulence, this quadratic approximation has been shown to be a good approximation for practical situations [17,18]. In oceanic turbulence, a significant difference between the new approach and quadratic approximation occurs in Fig. 1. It also demonstrates that some approaches valid in atmospheric turbulence while invalid in oceanic turbulence.

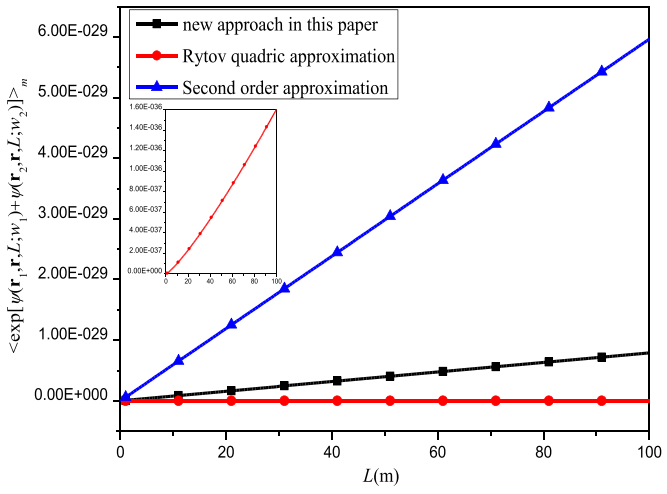

Fig. 1. Changes of $\left\langle \exp[\psi(\mathbf{r_1}, \mathbf{r}, L; \omega_1) + \psi^*(\mathbf{r_2}, \mathbf{r}, L; \omega_2)]\right\rangle_m$ versus the propagation length L.

4. Temporal broadening

4.1. Formulae

In this part, following Liu and Yeh [27], pulse statistics can be described using a temporal moment approach [16]. $\langle M^n(\mathrm{r}, L)\rangle$ denotes the nth moment and is given by

$$\langle M^n(\mathrm{r}, L)\rangle = \int_{-\infty}^{\infty} t^n\langle I(\mathrm{r}, L, t)\rangle \mathrm{d}t, \qquad n = 0, 1, 2, 3, \ldots \tag{12}$$

By using properties of the Dirac delta function [28]

$$\int_{-\infty}^{\infty} t^n \exp[i(\omega_2 - \omega_1)]\mathrm{d}t = 2\pi(-i)^n\delta^{(n)}(\omega_2 - \omega_1),$$
$$\int_{-\infty}^{\infty} \delta^{(n)}(\omega_2 - \omega_1)f(\omega_2)\mathrm{d}\omega_2 = (-1)^n\frac{\partial^n}{\partial\omega_2^n}f(\omega_2)|_{\omega_2=\omega_1}, \tag{13}$$

it can be shown that Eq. (12) is given by

$$\langle M^n(\mathrm{r}, L)\rangle = \frac{\mathrm{i}^n}{2\pi}\int_{-\infty}^{\infty} V_i(\omega_1) \frac{\partial^n}{\partial\omega_2^n}[V_i^*(\omega_2)\Gamma_2(\mathrm{r}, \mathrm{r}, L; \omega_1 + \omega_0, \omega_2 + \omega_0)]|_{\omega_2=\omega_1} \mathrm{d}\omega_1. \tag{14}$$

Based on the mentioned above temporal moments, each moment corresponds to a physical characteristic: the zeroth moment relates to the total energy of the pulse, the first moment relates to the mean arrival time and the second moment is related to the pulse width, etc. [2]. Assuming baseband $\omega_0 = 0$, the total energy of the pulse is

$$\langle M^{(0)}(\mathrm{r}, L)\rangle = \frac{1}{Q^2L^2c^2}\left[\sqrt{\pi A}Q + \pi\sqrt{PQ}\exp\left(\frac{AP}{Q}\right)\left(\mathrm{erf}\left[\sqrt{\frac{AP}{Q}}\right] - 1\right)\right], \tag{15}$$

where $A = T_0^2/2$, $P = 4/W_0^4$, $Q = 1/L^2c^2 - 4E/W_0^2$ and erf[•] is the error function.

The mean arrival time of the pulse is

$$\langle M^{(1)}(\mathrm{r}, L)\rangle = \frac{iA}{L^2c^2}\left\{\frac{(\pi/A)^{1/2}b_4}{Q^2} + (b_4P - b_2Q)\left[\frac{(\pi A)^{1/2}}{Q^3} - \frac{\pi AP^{1/2}}{Q^{7/2}}\exp\left(\frac{AP}{Q}\right)\left(\mathrm{erf}\left[\sqrt{\frac{AP}{Q}}\right] - 1\right)\right] + (3b_4P - b_2Q)\frac{\pi P^{-1/2}}{2Q^{5/2}}\exp\left(\frac{AP}{Q}\right)\left(\mathrm{erf}\left[\sqrt{\frac{AP}{Q}}\right] - 1\right)\right\}, \tag{16}$$

where $b_2 = -(2i/LcW_0^2 + 4iL/cW_0^4)$, $b_4 = iE/Lc - i/Lc^3 + 4iLE/cW_0^2$.

The pulse width is

$$\left\langle M^2(r, L)\right\rangle = \frac{\mathrm{i}^2AS}{L^2c^2}\left[\exp\left(\frac{AP}{Q}\right)\left(\mathrm{erf}\left[\sqrt{\frac{AP}{Q}}\right] - 1\right) + \sqrt{\frac{P}{Q}}\right], \tag{17}$$

where

$$S = \frac{(Q/P)^{3/2}}{8A^{3/2}Q^7}\{(\pi P/Q)^{1/2}[4h_5PQ^4 + 8g_5APQ^3 - 16h_5AP^2Q^3 + 8h_3APQ^4 + 4A^3PQ(g_5P^2 - g_3PQ + g_1Q^2) + 2A^2Q^2(9g_5P^2 - 4h_5P^3 - 5g_3PQ + 4h_3P^2Q + g_1Q^2 - 4h_1PQ^2)]\}, B = 1 - \frac{iL}{c}, R = \frac{D}{2} + \frac{T_0^2}{4}, t_0 = \frac{2i}{LcW_0^2}, t_1 = -\frac{2i}{LcW_0^2}, t_2 = \frac{iE}{Lc}, t_3 = -\frac{iE}{Lc}, \alpha = Pt_3, \beta = PD - t_1t_3 + 2t_0t_3 - 4PR, \gamma = 2Dt_0 - Dt_1 + 2Qt_3 + 2t_2 + 4Rt_1 - 6Rt_0, \xi = 2DQ - t_2t_3 - 6RQ, \delta = 2Rt_2 - Dt_2, h_1 = \beta B - \alpha A, h_3 = \xi B - \gamma A, h_5 = -\delta A, g_1 = 2\alpha Q + 2\beta t_0, g_3 = 2\gamma Q + 2\xi t_0 - 2\beta t_2, g_5 = -2\xi t_2 + 2\delta Q.$$

when $E = 0$ and $D = 0$, Eq. (17) reduces to the pulse width in free space $\langle M^2_{Free}\rangle$.

4.2. Numerical calculation results and analysis

The Rytov variance in oceanic turbulence is an indispensable quantity that can distinguish the weak, moderate and strong fluctuation oceanic turbulent conditions, and the quantity is widely used as a measure of the strength of turbulence [12,16]. Until now, there has been no paper concerning how to distinguish the oceanic turbulent strength quantitatively. In this paper, similar to the Rytov variance in atmospheric turbulence [16], the expression of Rytov variance in oceanic turbulent case is obtained, i.e., $\sigma_R^2 = 3.063 \times 10^{-7}k^{7/6}L^{11/6}\varepsilon^{-1/3}\frac{\chi_T}{w^2}(0.358w^2 - 0.725w + 0.367)$ (see Appendix in this paper). As we know, free space, weak, moderate and strong turbulence are associated with $\sigma_R^2 = 0$, $\sigma_R^2 < 1$, $\sigma_R^2 \sim 1$, and $\sigma_R^2 > 1$, respectively (see Chapter 5 in Ref. [16]). In this section, on-axis relative pulse broadening of pulses versus propagation length in the moderate turbulence is investigated. The extension to arbitrary turbulent strength is straightforward. Then, four Rytov variance (i.e., $\sigma_R^2 = 0$, $\sigma_R^2 = 0.5$, $\sigma_R^2 = 1$ and $\sigma_R^2 = 2$, respectively), $L = 50$m and $\lambda = 0.417\mu$m are chosen. In Figs. 3–6 the on-axis relative broadening of pulse (i.e., $\langle M^2(0, L)\rangle/2T_0$) and the turbulent effective coefficient (i.e., $\langle M^2_{Turb}\rangle/\langle M^2_{Free}\rangle$) are investigated.

Fig. 2 shows on-axis relative pulse broadening of pulses versus propagation length with various wavelength. Given the fixed initial Gaussian beam radius and initial pulse half-width, it is shown that the on-axis relative pulse broadening increases as the propagation length increases. Besides, the larger wavelength determines the wider pulse broadening.

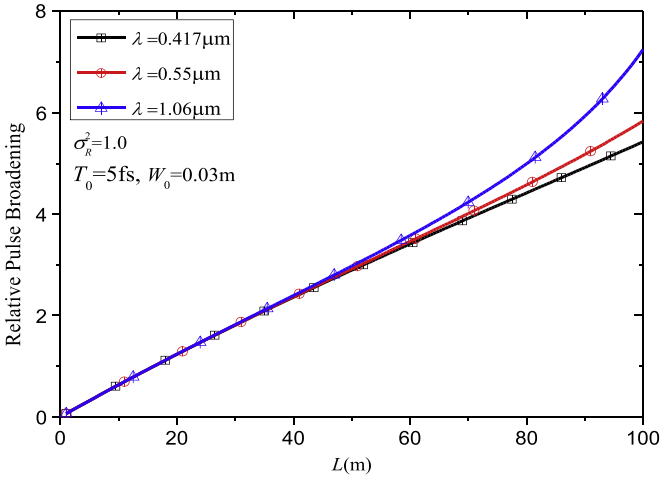

Fig. 2. On-axis relative pulse broadening versus propagation length L.

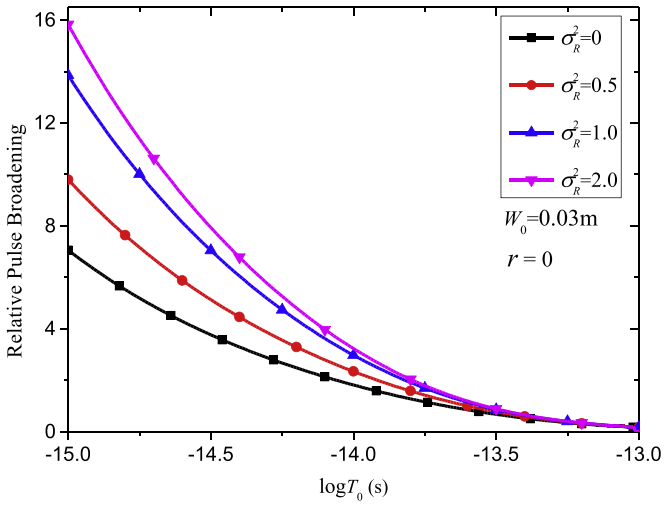

Fig. 3. On-axis relative pulse broadening versus the logarithm of initial pulse half-width $\log T_0$.

Fig. 3 shows on-axis relative pulse broadening of pulses versus the logarithm of initial pulse half-width in the femtosecond–picosecond regime. Given the fixed initial Gaussian beam radius, it is shown that the on-axis relative pulse broadening decreases as the initial pulse half-width increases in free space, weak, moderate and strong turbulent regions. The stronger oceanic turbulence determines the wider pulse broadening.

The relation between on-axis relative pulse broadening and initial beam radius is investigated in Fig. 4. Fig. 4 shows that the value of initial beam radius determines on-axis relative pulse broadening. It is shown that the higher value of W_0 leads to wider pulse broadening in various strength of turbulence.

In this paper, the on-axis turbulent effective coefficient is defined as the ratio of pulse width in turbulent ocean to pulse width in free space. This quantity is described as the single factor of pulse broadening by oceanic turbulence. Fig. 5 shows the on-axis turbulent effective coefficient versus the logarithm of initial pulse half-width in the femtosecond–picosecond regime. It is shown that the value of on-axis turbulent effective coefficient in weak fluctuation turbulence is the lowest. The pulse broadening is less affected in weak turbulence compared to that in moderate and strong cases.

Fig. 6 shows the on-axis turbulent effective coefficient versus the initial beam radius. It is also shown that the value of on-axis

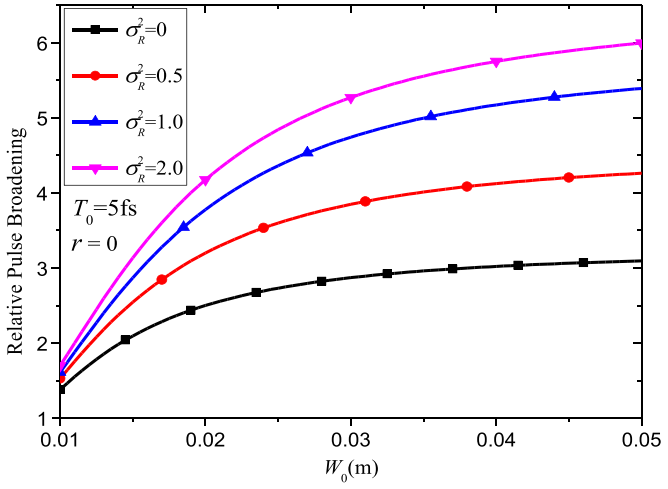

Fig. 4. On-axis relative pulse broadening versus initial Gaussian beam radius W_0.

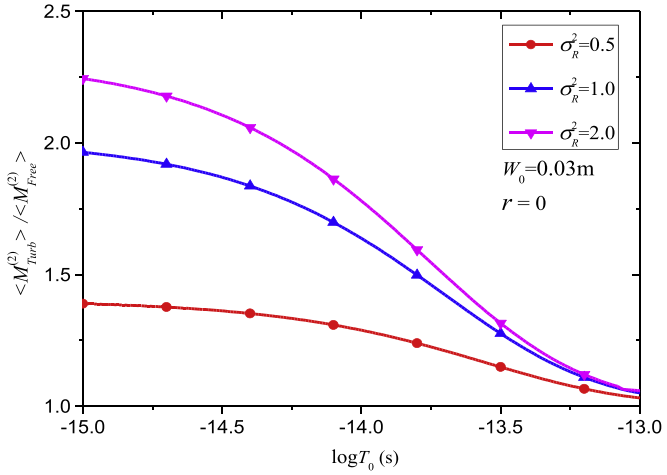

Fig. 5. On-axis turbulent effective coefficient versus the logarithm of initial pulse half-width log T_0.

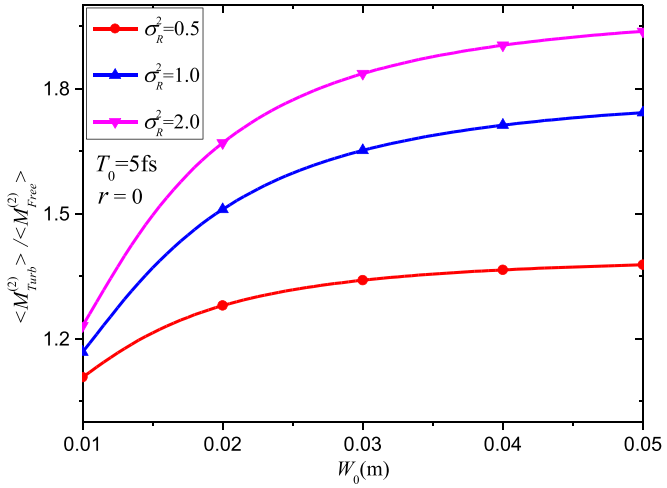

Fig. 6. On-axis turbulent effective coefficient versus initial Gaussian beam radius W_0.

turbulent effective coefficient in weak fluctuation turbulence is the lowest. The pulse broadening is less affected in weak turbulence compared to that in moderate and strong cases.

5. Conclusions

In this paper, the results of three approaches of the correlation function of the complex phase perturbed by oceanic turbulence is shown. It is clear that a significant difference among three approaches occurs: the new approach is much smaller than the second order approximation and close to quadratic approximation. The analytical expression for two-frequency mutual coherence function (MCF) of ultra-short pulses propagating through oceanic turbulence is obtained. Based on the two-frequency MCF, the analytical expression of pulse width of optical pulses transmitting through oceanic turbulence is derived. In arriving at the results, using a temporal moments approach and combining with the expression for the MCF, the analytical expression for the pulse width is deduced. Based on the quantity of Rytov variance in oceanic turbulence, we investigate the changes of on-axis relative pulse broadening of ultra-short pulses with propagation length, wavelength initial pulse half-width and initial Gaussian beam radius from free space to strong turbulent regions. It is shown that the on-axis relative pulse broadening decreases as initial pulse half-width increases, and increases as propagation length, wavelength and initial Gaussian beam radius increases. The on-axis turbulent effective coefficient is also studied. It is shown that the pulse broadening is less affected in weak fluctuation condition compared to that in moderate and strong cases. Besides, to different turbulent strength, we obtain that the broadening of ultra-short pulse in strong turbulence is much wider than that of weak and moderate conditions. We believe that our work must be useful in laser applications, such as, ultra-short femtosecond pulsed laser technology, laser pulse communication system and etc.

Acknowledgments

The authors are very thankful to the reviewers and editors for valuable comments. All authors acknowledge the support by the National Natural Science Foundation of China (NSFC) under Grant 61405205 and 61475105.

Appendix. : Analytical formulae of the Rytov variance in oceanic turbulence

Based on Ref. [16], the Rytov variance for a plane wave is given as

$$\sigma_R^2 = 8\pi^2 k^2 L \int_0^1 \int_0^\infty \kappa \Phi_n(\kappa)\left[1 - \cos\left(\frac{L\kappa^2\xi}{k}\right)\right]\mathrm{d}\kappa\mathrm{d}\xi, \tag{18}$$

on subtracting the relation [28] $\cos x = (-1)^n x^{2n}/(2n)!$ into Eq. (18), the Rytov variance is expressed as

$$\sigma_R^2 = 8\pi^2 k^2 L \sum_{n=1}^{\infty} \int_0^1 \xi^2 \mathrm{d}\xi \int_0^\infty \frac{(-1)^{n+1} L^{2n}\kappa^{4n+1}\Phi_n(\kappa)}{k^{2n}(2n)!}\mathrm{d}\kappa, \tag{19}$$

Based on the power spectrum for oceanic turbulence and the integrals in Ref. [29],

$$\begin{aligned}&\int_0^\infty \kappa^{2n-\frac{8}{3}} e^{-Q\kappa^{\frac{4}{3}}-R\kappa^2}\mathrm{d}\kappa \\ &= \frac{1}{4}R^{-\frac{1}{2}-n}\left\{2R^{\frac{4}{3}}\Gamma\left(n-\frac{5}{6}\right){}_2F_2\left(\frac{n}{2}-\frac{5}{12},\frac{n}{2}+\frac{1}{12};\frac{1}{3},\frac{2}{3};-\frac{4Q^3}{27R^2}\right)\right. \\ &\quad - 2QR^{\frac{2}{3}}\Gamma\left(n-\frac{1}{6}\right){}_2F_2\left(\frac{n}{2}-\frac{1}{12},\frac{n}{2}+\frac{5}{12};\frac{2}{3},\frac{4}{3};-\frac{4Q^3}{27R^2}\right) \\ &\quad \left.+ Q^2\Gamma\left(n+\frac{1}{2}\right){}_2F_2\left(\frac{n}{2}+\frac{1}{4},\frac{n}{2}+\frac{3}{4};\frac{4}{3},\frac{5}{3};-\frac{4Q^3}{27R^2}\right)\right\},\end{aligned} \tag{20}$$

$$\begin{aligned}\int_0^\infty \kappa^{2n-2} e^{-Q\kappa^{\frac{4}{3}}-R\kappa^2}\mathrm{d}\kappa = \frac{1}{4}R^{-\frac{5}{6}-n}\{&2R^{\frac{4}{3}}\Gamma\left(n-\frac{1}{2}\right){}_2F_2\left(\frac{n}{2}-\frac{1}{4},\frac{n}{2}+\frac{1}{4};\frac{1}{3},\frac{2}{3};-\frac{4Q^3}{27R^2}\right) \\ &- 2QR^{\frac{2}{3}}\Gamma\left(n+\frac{1}{6}\right){}_2F_2\left(\frac{n}{2}+\frac{1}{12},\frac{n}{2}+\frac{7}{12};\frac{2}{3},\frac{4}{3};-\frac{4Q^3}{27R^2}\right) \\ &+ Q^2\Gamma\left(n+\frac{5}{6}\right){}_2F_2\left(\frac{n}{2}+\frac{5}{12},\frac{n}{2}+\frac{11}{12};\frac{4}{3},\frac{5}{3};-\frac{4Q^3}{27R^2}\right)\},\end{aligned} \tag{21}$$

where $\Gamma(\bullet)$ is the Gamma function and ${}_pF_q(a_1, \ldots, a_p; c_1, \ldots c_q; x)$is the generalized hypergeometric function, where p and q are positive integers.

Subtracting Eqs. (1), (20) and (21) into Eq. (19), the Rytov variance for a plane wave is given as

where $a = 8.284A_T\eta^{4/3}$, $b = 12.978A_T\eta^2$, $c = 8.284A_S\eta^{4/3}$, $d = 12.978A_S\eta^2$, $e = 8.284A_{TS}\eta^{4/3}$ $f = 12.978A_{TS}\eta^2$ and $g = 2.35\eta^{2/3}$.

For power spectrum in Eq. (1), we have proved that $\frac{4Q^3}{27R^2} \ll 1$ (Q=a, c, e; R=b, d, f) is always satisfied. Thus, for our case we can

simplify the integration result from Eq. (22) by using the following formula for the $|x| \ll 1$case [26], i.e.

$$ {}_2F_2(\alpha, \beta; \gamma, \varsigma; -x) = 1 - \frac{\alpha\beta x}{\gamma\varsigma}, \ |x| \ll 1 \tag{23}$$

applying the definition of Pochhammer symbol [16] (i.e., $(a)_n = \Gamma(a+n)/\Gamma(a)$, $(n = 1, 2, 3, \ldots)$) and recurrence relations [16] (i.e., $(a+n)(a)_n = a(1+a)_n$ and $(a)_{2n} = 2^{2n}(a/2)_n(1/2 + a/2)_n$), the Eq. (22) can be expressed as

$$\begin{aligned}
\sigma_R^2 = {} & 0.388 \times 10^{-6} \times 8\pi^2 k^2 L \varepsilon^{-1/3} \frac{\chi_T}{w^2} \\
& \times \left\{ \frac{1}{2} b^{5/6} \Gamma\left(-\frac{5}{6}\right)\left(1 - \frac{91a^3}{216b^2}\right) w^2 \sum_{n=1}^{\infty} \frac{(-1)^{n+1} L^{2n} (-5/12)_n (1/12)_n}{k^{2n} b^{2n} (3/2)_n (n!)} \right. \\
& + \frac{1}{2} d^{5/6} \Gamma\left(-\frac{5}{6}\right)\left(1 - \frac{91c^3}{216d^2}\right) \sum_{n=1}^{\infty} \frac{(-1)^{n+1} L^{2n} (-5/12)_n (1/12)_n}{k^{2n} d^{2n} (3/2)_n (n!)} \\
& - f^{5/6} \Gamma\left(-\frac{5}{6}\right)\left(1 - \frac{91e^3}{216f^2}\right) w \sum_{n=1}^{\infty} \frac{(-1)^{n+1} L^{2n} (-5/12)_n (1/12)_n}{k^{2n} f^{2n} (3/2)_n (n!)} \\
& - ab^{-1/6} \Gamma\left(-\frac{5}{6}\right)\left(1 - \frac{247a^3}{864b^2}\right) w^2 g \sum_{n=1}^{\infty} \frac{(-1)^{n+1} L^{2n} (1/12)_n (7/12)_n}{k^{2n} b^{2n} (3/2)_n (n!)} \\
& - cd^{-1/6} \Gamma\left(-\frac{5}{6}\right)\left(1 - \frac{247c^3}{864d^2}\right) g \sum_{n=1}^{\infty} \frac{(-1)^{n+1} L^{2n} (1/12)_n (7/12)_n}{k^{2n} d^{2n} (3/2)_n (n!)} \\
& + 2ef^{-1/6} \Gamma\left(-\frac{5}{6}\right)\left(1 - \frac{247e^3}{864f^2}\right) wg \sum_{n=1}^{\infty} \frac{(-1)^{n+1} L^{2n} (1/12)_n (7/12)_n}{k^{2n} f^{2n} (3/2)_n (n!)} \\
& + \frac{1}{2} b^{1/2} \Gamma\left(-\frac{1}{2}\right)\left(1 - \frac{5a^3}{8b^2}\right) w^2 \sum_{n=1}^{\infty} \frac{(-1)^{n+1} L^{2n} (-1/4)_n (1/4)_n}{k^{2n} b^{2n} (3/2)_n (n!)} \\
& + \frac{1}{2} d^{1/2} \Gamma\left(-\frac{1}{2}\right)\left(1 - \frac{5c^3}{8d^2}\right) \sum_{n=1}^{\infty} \frac{(-1)^{n+1} L^{2n} (-1/4)_n (1/4)_n}{k^{2n} d^{2n} (3/2)_n (n!)} \\
& - f^{1/2} \Gamma\left(-\frac{1}{2}\right)\left(1 - \frac{5e^3}{8f^2}\right) w \sum_{n=1}^{\infty} \frac{(-1)^{n+1} L^{2n} (-1/4)_n (1/4)_n}{k^{2n} f^{2n} (3/2)_n (n!)} \\
& + \frac{1}{2} a^2 b^{-1/2} \Gamma\left(-\frac{1}{2}\right)\left(\frac{3}{2}\right)_n \left(1 - \frac{7a^3}{48b^2}\right) w^2 g \sum_{n=1}^{\infty} \frac{(-1)^{n+1} L^{2n} (1/4)_n (3/4)_n}{k^{2n} b^{2n} (3/2)_n (n!)} \\
& + \frac{1}{2} c^2 d^{-1/2} \Gamma\left(-\frac{1}{2}\right)\left(\frac{3}{2}\right)_n \left(1 - \frac{7c^3}{48d^2}\right) g \sum_{n=1}^{\infty} \frac{(-1)^{n+1} L^{2n} (1/4)_n (3/4)_n}{k^{2n} d^{2n} (3/2)_n (n!)} \\
& - e^2 f^{-1/2} \Gamma\left(-\frac{1}{2}\right)\left(\frac{3}{2}\right)_n \left(1 - \frac{7e^3}{48f^2}\right) wg \sum_{n=1}^{\infty} \frac{(-1)^{n+1} L^{2n} (1/4)_n (3/4)_n}{k^{2n} f^{2n} (3/2)_n (n!)} \\
& - \frac{1}{2} ab^{1/6} \Gamma\left(-\frac{1}{6}\right)\left(1 - \frac{187a^3}{864b^2}\right) w^2 \sum_{n=1}^{\infty} \frac{(-1)^{n+1} L^{2n} (-1/12)_n (5/12)_n}{k^{2n} b^{2n} (3/2)_n (n!)} \\
& - \frac{1}{2} cd^{1/6} \Gamma\left(-\frac{1}{6}\right)\left(1 - \frac{187c^3}{864d^2}\right) \sum_{n=1}^{\infty} \frac{(-1)^{n+1} L^{2n} (-1/12)_n (5/12)_n}{k^{2n} d^{2n} (3/2)_n (n!)} \\
& + ef^{1/6} \Gamma\left(-\frac{1}{6}\right)\left(1 - \frac{187e^3}{864f^2}\right) w \sum_{n=1}^{\infty} \frac{(-1)^{n+1} L^{2n} (-1/12)_n (5/12)_n}{k^{2n} f^{2n} (3/2)_n (n!)} \\
& + \frac{1}{2} a^2 b^{-5/6} \Gamma\left(-\frac{1}{6}\right)\left(1 - \frac{391a^3}{2160b^2}\right) w^2 g \sum_{n=1}^{\infty} \frac{(-1)^{n+1} L^{2n} (5/12)_n (11/12)_n}{k^{2n} b^{2n} (3/2)_n (n!)} \\
& + \frac{1}{2} c^2 d^{-5/6} \Gamma\left(-\frac{1}{6}\right)\left(1 - \frac{391c^3}{2160d^2}\right) g \sum_{n=1}^{\infty} \frac{(-1)^{n+1} L^{2n} (5/12)_n (11/12)_n}{k^{2n} d^{2n} (3/2)_n (n!)} \\
& \left. - e^2 f^{-5/6} \Gamma\left(-\frac{1}{6}\right)\left(1 - \frac{391e^3}{2160f^2}\right) wg \sum_{n=1}^{\infty} \frac{(-1)^{n+1} L^{2n} (5/12)_n (11/12)_n}{k^{2n} f^{2n} (3/2)_n (n!)} \right\},
\end{aligned} \tag{24}$$

applying the definition of the hypergeometric function (see Appendix I in [16], i.e., ${}_2F_1(a_1, b_1; c_1; z) = \sum_{n=0}^{\infty} \frac{(a_1)_n (b_1)_n}{(c_1)_n} \frac{z^n}{n!}$, $|z| \ll \infty$) Eq. (24) can be expressed as

$$\begin{aligned}
\sigma_R^2 = {} & 0.388 \times 10^{-6} \times 8\pi^2 k^2 L \varepsilon^{-1/3} \frac{\chi_T}{w^2} \left\{ \frac{1}{2} b^{5/6} \Gamma\left(-\frac{5}{6}\right)\left(1 - \frac{91a^3}{216b^2}\right) w^2 \right. \\
& \left[1 - {}_2F_1\left(-\frac{5}{12}, \frac{1}{12}; \frac{3}{2}; -\frac{L^2}{k^2 b^2}\right) \right] \\
& + \frac{1}{2} d^{5/6} \Gamma\left(-\frac{5}{6}\right)\left(1 - \frac{91c^3}{216d^2}\right)\left[1 - {}_2F_1\left(-\frac{5}{12}, \frac{1}{12}; \frac{3}{2}; -\frac{L^2}{k^2 d^2}\right) \right] \\
& - f^{5/6} \Gamma\left(-\frac{5}{6}\right)\left(1 - \frac{91e^3}{216f^2}\right) w \left[1 - {}_2F_1\left(-\frac{5}{12}, \frac{1}{12}; \frac{3}{2}; -\frac{L^2}{k^2 f^2}\right) \right] \\
& - ab^{-1/6} \Gamma\left(-\frac{5}{6}\right)\left(1 - \frac{247a^3}{864b^2}\right) w^2 g \left[1 - {}_2F_1\left(\frac{1}{12}, \frac{7}{12}; \frac{3}{2}; -\frac{L^2}{k^2 b^2}\right) \right] \\
& - cd^{-1/6} \Gamma\left(-\frac{5}{6}\right)\left(1 - \frac{247c^3}{864d^2}\right) g \left[1 - {}_2F_1\left(\frac{1}{12}, \frac{7}{12}; \frac{3}{2}; -\frac{L^2}{k^2 d^2}\right) \right] \\
& + 2ef^{-1/6} \Gamma\left(-\frac{5}{6}\right)\left(1 - \frac{247e^3}{864f^2}\right) wg \left[1 - {}_2F_1\left(\frac{1}{12}, \frac{7}{12}; \frac{3}{2}; -\frac{L^2}{k^2 f^2}\right) \right] \\
& + \frac{1}{2} b^{1/2} \Gamma\left(-\frac{1}{2}\right)\left(1 - \frac{5a^3}{8b^2}\right) w^2 \left[1 - {}_2F_1\left(-\frac{1}{4}, \frac{1}{4}; \frac{3}{2}; -\frac{L^2}{k^2 b^2}\right) \right] \\
& + \frac{1}{2} d^{1/2} \Gamma\left(-\frac{1}{2}\right)\left(1 - \frac{5c^3}{8d^2}\right)\left[1 - {}_2F_1\left(-\frac{1}{4}, \frac{1}{4}; \frac{3}{2}; -\frac{L^2}{k^2 d^2}\right) \right] \\
& - f^{1/2} \Gamma\left(-\frac{1}{2}\right)\left(1 - \frac{5e^3}{8f^2}\right) w \left[1 - {}_2F_1\left(-\frac{1}{4}, \frac{1}{4}; \frac{3}{2}; -\frac{L^2}{k^2 f^2}\right) \right] \\
& + \frac{1}{2} a^2 b^{-1/2} \Gamma\left(-\frac{1}{2}\right)\left(\frac{3}{2}\right)_n \left(1 - \frac{7a^3}{48b^2}\right) w^2 g \left[1 - {}_2F_1\left(\frac{1}{4}, \frac{3}{4}; \frac{3}{2}; -\frac{L^2}{k^2 b^2}\right) \right] \\
& + \frac{1}{2} c^2 d^{-1/2} \Gamma\left(-\frac{1}{2}\right)\left(\frac{3}{2}\right)_n \left(1 - \frac{7c^3}{48d^2}\right) g \left[1 - {}_2F_1\left(\frac{1}{4}, \frac{3}{4}; \frac{3}{2}; -\frac{L^2}{k^2 d^2}\right) \right] \\
& - e^2 f^{-1/2} \Gamma\left(-\frac{1}{2}\right)\left(\frac{3}{2}\right)_n \left(1 - \frac{7e^3}{48f^2}\right) wg \left[1 - {}_2F_1\left(\frac{1}{4}, \frac{3}{4}; \frac{3}{2}; -\frac{L^2}{k^2 f^2}\right) \right] \\
& - \frac{1}{2} ab^{1/6} \Gamma\left(-\frac{1}{6}\right)\left(1 - \frac{187a^3}{864b^2}\right) w^2 \left[1 - {}_2F_1\left(-\frac{1}{12}, \frac{5}{12}; \frac{3}{2}; -\frac{L^2}{k^2 b^2}\right) \right] \\
& - \frac{1}{2} cd^{1/6} \Gamma\left(-\frac{1}{6}\right)\left(1 - \frac{187c^3}{864d^2}\right)\left[1 - {}_2F_1\left(-\frac{1}{12}, \frac{5}{12}; \frac{3}{2}; -\frac{L^2}{k^2 d^2}\right) \right] \\
& + ef^{1/6} \Gamma\left(-\frac{1}{6}\right)\left(1 - \frac{187e^3}{864f^2}\right) w \left[1 - {}_2F_1\left(-\frac{1}{12}, \frac{5}{12}; \frac{3}{2}; -\frac{L^2}{k^2 f^2}\right) \right] \\
& + \frac{1}{2} a^2 b^{-5/6} \Gamma\left(-\frac{1}{6}\right)\left(1 - \frac{391a^3}{2160b^2}\right) w^2 g \left[1 - {}_2F_1\left(\frac{5}{12}, \frac{11}{12}; \frac{3}{2}; -\frac{L^2}{k^2 b^2}\right) \right] \\
& + \frac{1}{2} c^2 d^{-5/6} \Gamma\left(-\frac{1}{6}\right)\left(1 - \frac{391c^3}{2160d^2}\right) g \left[1 - {}_2F_1\left(\frac{5}{12}, \frac{11}{12}; \frac{3}{2}; -\frac{L^2}{k^2 d^2}\right) \right] \\
& \left. - e^2 f^{-5/6} \Gamma\left(-\frac{1}{6}\right)\left(1 - \frac{391e^3}{2160f^2}\right) wg \left[1 - {}_2F_1\left(\frac{5}{12}, \frac{11}{12}; \frac{3}{2}; -\frac{L^2}{k^2 f^2}\right) \right] \right\},
\end{aligned} \tag{25}$$

Subtracting the fixed parameters, the Rytov variance is simplified as

$$\sigma_R^2 = 3.063 \times 10^{-7} k^{7/6} L^{11/6} \varepsilon^{-1/3} \chi_T \left(0.358w^2 - 0.725w + 0.367\right)/w^2. \tag{26}$$

References

[1] D.E. TjinThamSjin Kelly, L.C. Andrews, Waves Random Media 9 (1999) 307.
[2] C.Y. Young, Proc. SPIE 4821 (2002) 74–81.
[3] C. Chen, H. Yang, Y. Lou, S. Tong, R. Liu, Opt. Express 20 (7) (2012) 7749.
[4] C. Chen, H. Yang, S. Tong, B. Ren, Y. Li, Opt. Express 23 (4) (2015) 4814–4828.
[6] S.H. Choi, U. Osterberg, Phys. Rev. Lett. 92 (19) (2004) 193903.
[5] W.K. George, V.S. Alexei, Ultrashort Laser Pulse Propagation in Water, ⟨http://people.physics.tamu.edu/trouble/work.html⟩.
[7] S.T. Hong, A. Ishimaru, Radio Sci. 11 (1976) 551.
[8] I. Sreenivasiah, A. Ishimaru, S.T. Hong, Radio Sci. 11 (1976) 775.
[9] I. Sreenivasiah, A. Ishimaru, Appl. Opt. 18 (1979) 1613.
[10] R. LFante, J. Opt. Soc. Am. A 71 (1981) 1446.
[11] C.Y. Young, A. Ishimaru, L.C. Andrews, Appl. Opt. 35 (1996) 6522.
[12] C.Y. Young, L.C. Andrews, A. Ishimaru, Appl. Opt. 37 (33) (1998) 7655.
[13] V.V. Nikishovand, V.I. Nikishov, Int. J. Fluid Mech. Res. 27 (1) (2000) 82.
[14] W. Lu, L. Liu, J. Sun, J. Opt. A: Pure Appl. Opt. 8 (2006) 1052.
[15] N. Farwell, O. Korotkova, Opt. Commun. 285 (6) (2012) 872.

[16] L.C. Andrews, R.L. Phillips, Laser Beam Propagation through Random Media, SPIE, 2005.
[17] S.C.H. Wang, M.A. Plonus, J. Opt. Soc. Am. 69 (1979) 1297.
[18] J.C. Leader, J. Opt. Soc. Am. 68 (1978) 175.
[19] J.C. Ricklin, F.M. Davidson, J. Opt. Soc. Am. A 19 (2002) 1794.
[20] M. Salem, O. Korotkova, A. Dogariu, E. Wolf, Waves Random Media 14 (2004) 513.
[21] H.T. Eyyuboğlu, S. Altay, Y. Baykal, Opt. Commun. 264 (2006) 25.
[22] X. Chu, Z. Liu, Y. Wu, J. Opt. Soc. Am. A 25 (2008) 74.
[23] F. Chen, Q. Zhao, Y. Chen, J. Chen, J. Opt. Soc. Korea 17 (2013) 130–135.
[24] W. Fu, H. Zhang, Opt. Commun. 304 (2013) 11.
[25] O. Korotkova, N. Farwell, Opt. Commun. 284 (2011) 1740.
[26] L.C. Andrews, Special Functions of Mathematics for Engineers, 3rd ed., SPIE and Oxford University, 1998.
[27] C.H. Liu, K.C. Yeh, IEEE Trans. Antennas Propag. AP-26 (1978) 561.
[28] I.S. Gradshteyn, I.M. Ryzhik, Table of Integrals, Series, and Products, Seventh Edition, Academic press, 2007.
[29] L. Lu, X.L. Ji, Y. Baykal, Opt. Express 22 (2014) 27112.